Cells Tissues Organs

Cells Tissues Organs
DOI: 10.1159/000151724

Published online: August 26, 2008

Phosphorylation of Osteopontin Peptides Mediates Adsorption to and Incorporation into Calcium Oxalate Crystals

Jason O'Young[a] Sara Chirico[a] Nehal Al Tarhuni[a] Bernd Grohe[a]
Mikko Karttunen[b] Harvey A. Goldberg[a] Graeme K. Hunter[a]

[a]School of Dentistry and CIHR Group in Skeletal Development and Remodeling and
[b]Department of Applied Mathematics, University of Western Ontario, London, Ont., Canada

Key Words
Biomineralization · Kidney stones · Osteopontin · Confocal microscopy · Molecular dynamics

Abstract
Phosphorylated peptides of osteopontin (OPN) have been shown to inhibit the growth of the {100} face of calcium oxalate monohydrate (COM). The inhibitory potency has been shown to be dependent on the phosphate content of the peptide. The purpose of this study is to better understand the means by which phosphate groups promote crystal growth inhibition by OPN peptides. Peptides of rat bone OPN 220–235 peptides have been synthesized with zero (P0), 1 (P1) or 3 (P3) phosphate modifications. COM crystals were grown in the presence of 0.1–10 μg of P0, P1 or P3. P0 incorporation into COM crystals was evident at 10 μg/ml of peptide, whereas the phosphorylated peptides P1 and P3 were incorporated at all tested concentrations. At 5 μg/ml of P3, COM crystals exhibited a 'dumbbell' morphology. To study the peptide-mineral interaction, surface frequency plots were constructed from molecular dynamics simulations of OPN peptide adsorption. Carboxylate and phosphate groups were found to adsorb in specific orientations to the COM {100} surface. In conclusion, it appears that the phosphate groups on OPN peptides are capable of interacting with the COM {100} surface. This interaction appears to increase the adsorption energy of the peptide to the surface, thus enhancing its inhibitory potency.

Abbreviations used in this paper

COM	calcium oxalate monohydrate
MD	molecular dynamics
OPN	osteopontin

Introduction

Controlled mineralization in biological organisms is achieved in part by specifically modulating the growth of mineral phases. A proposed mechanism is that macromolecules present in solution are capable of directing crystal morphology by adsorbing to specific crystal features. It is generally accepted that, in solution, crystal faces grow by the diffusion and subsequent adsorption of ions to a crystal surface or kink site [Burton et al., 1951]. The adsorption of a macromolecular additive to a growing crystal face can inhibit the attachment of ions by occupying potential adsorption sites. Through this mechanism, organisms can control the kinetics and growth habits of biominerals.

Calcium oxalate monohydrate (COM) is the major inorganic component of kidney stones [Coe et al., 1992].

KARGER

Fax +41 61 306 12 34
E-Mail karger@karger.ch
www.karger.com

1422–6405/08/0000–0000$24.50/0

Accessible online at:
www.karger.com/cto

Dr. Graeme K. Hunter
CIHR Group in Skeletal Development and Remodeling
Schulich School of Medicine and Dentistry, University of Western Ontario
London, ON N6A 5C1 (Canada)
Tel. +1 519 661 2185, Fax +1 519 850 2459, E-Mail graeme.hunter@schulich.uwo.ca

Table 1. Rat bone OPN phosphopeptides

Peptide name	Peptide sequence
P0 (OPN 220–235)	SHESTEQDAIDSAEK
P1 (OPN 220–235)	SHESTEQDAID**pS**AEK
P3 (OPN 220–235)	**pS**HE**pS**TEQDAID**pS**AEK
OPN 44–56	SV**pSpS**EE**pT**DDFKQE
OPN 60–75	**pS**N**pS**NE**pS**HDHMDDDDDD
OPN 152–167	DA**pT**DEDLT**pS**RMK**pS**QE**pS**
OPN 193–208	**pS**HE**pS**SQLDEP**pS**VETHS
OPN 257–270	**pS**LEHQ**pS**HEFH**pS**HED
OPN 290–301	**pS**HELE**pSpSpS**SEVN

Previous studies have shown that in vitro COM crystallization is significantly more inhibited by urinary proteins from normal compared to stone-forming subjects [Nakagawa et al., 1983]. This suggests a protective role for urinary proteins against urolithiasis.

Osteopontin (OPN) is a urinary protein that has been shown to inhibit the in vitro crystallization of COM [Shiraga et al., 1992; Hoyer et al., 2001]. OPN knockout mice have been shown to have a higher susceptibility to ethylene glycol-induced urolithiases [Wesson et al., 2003]. Additionally, adsorption of OPN directly on COM crystals has been demonstrated [Taller et al., 2007]. COM crystals grown in the presence of OPN also demonstrate a severely modified growth habit [Taller et al., 2007].

We have synthesized peptides of rat bone OPN (220–235) with different degrees of phosphorylation (P0, P1, P3) and have shown that these adsorb specifically to the {100} face of COM [Grohe et al., 2007]. However, the degree to which the growth of the {100} face was inhibited by these peptides was shown to be dependent on the degree of phosphorylation [Grohe et al., 2007]. This finding is in agreement with previous studies showing that synthetic phosphopeptides of OPN are more potent inhibitors of COM growth than the corresponding nonphosphorylated peptides [Hoyer et al., 2001]. Molecular dynamics (MD) simulations have suggested that phosphorylation increases peptide attraction to the crystal surface, which is permissive to the formation of strong electrostatic contacts between peptide residues and the surface [Grohe et al., 2007]. However, a surface characterization of the peptide-crystal interaction has not been performed. Knowledge of surface adsorption profiles is important in the design of peptides with specific surface adsorption activity [Capriotti et al., 2007].

Previous research has shown the incorporation of fluorescent molecules and proteins in COM single crystals [Touryan et al., 2001]. In the present study, we have used confocal microscopy to study the incorporation behaviors of 3 previously characterized rat OPN peptides (P0, P1, P3) into COM crystals. Additionally, we have used MD simulations to investigate the adsorptive characteristics of the {100} surface of COM. By these methods, we hope to provide an atomic-scale mechanism for increased growth modulation observed due to phosphorylation.

Materials and Methods

Analysis of the Incorporation of Phosphorylated OPN Peptides in COM Crystals

Residues 220–235 of rat bone OPN were synthesized (table 1) and labeled with Alexa Fluor 488 (Invitrogen) as previously described [Taller et al., 2007].

Growth of COM crystals was initiated as previously described [Taller et al., 2007] and the crystals grown for 30 min in the presence of 0.1, 1.0, 5.0 or 10.0 μg/ml of labeled peptide. Confocal microscopic images (Carl Zeiss LSM 510) were acquired as previously described [Taller et al., 2007]. All images were captured from the green channel with the focal plane set at 1.0 μm.

Analysis of the COM {100} Surface

MD simulations of COM {100} face adsorption were performed with P0, P1 and P3 as previously described [Grohe et al., 2007]. Additional 5-ns simulations were run for 6 other OPN sequences (table 1). The posttranslational modifications of the sequences were previously elucidated [Keykhosravani et al., 2005]. To determine the adsorptive topology of the surface, a 1-angstrom-thick slab residing on the outermost surface atoms was defined. The slab was further divided into sections of 0.5208 × 0.5058 Å in the plane of the surface. The thickness of the sections was equal to the thickness of the slab (1 Å). This resulted in a two-dimensional 'grid' of 168 × 120 sections in the plane of the surface. To determine the surface frequency of atoms residing at the surface, the atom type within each cube was recorded for every time point sampled. Trajectories were sampled every picosecond. Solvent atoms were excluded from the calculation. The frequencies for each 'unit plane' and all trajectories were added. Overall, this calculation serves to identify the most frequented areas of the surface by adsorbate atoms.

Results

COM crystals grown in the presence of the P0 peptide showed very slight crystal incorporation at 0.1, 1.0 and 5.0 μg/ml of peptide (fig. 1a). At these concentrations, the majority of fluorescent signals was found at the {100}-solution interface. At 10 μg/ml, there is evident incorporation of P0 into the crystal. The fluorescence followed a pattern that is identical to the expected growth pattern of

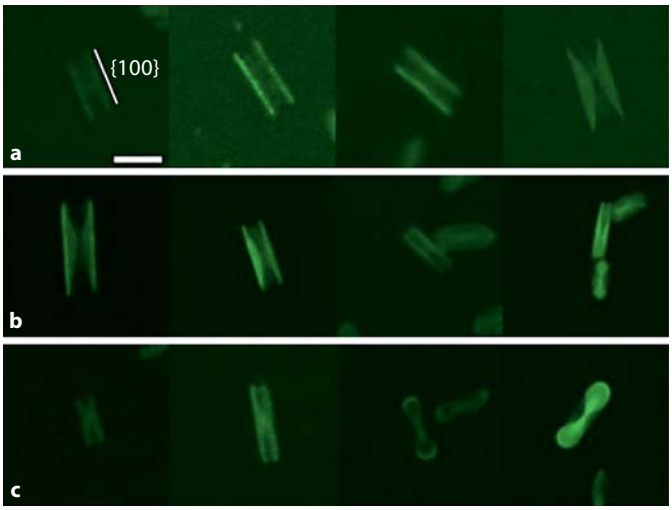

Fig. 1. Fluorescence imaging of OPN peptide incorporation into COM crystals. **a** P0 peptide. **b** P1 peptide. **c** P3 peptide. Initial peptide concentrations are indicated. All crystals are nucleated from {010} and are imaged approximately midway through the crystal. Scale bar = 10 µm.

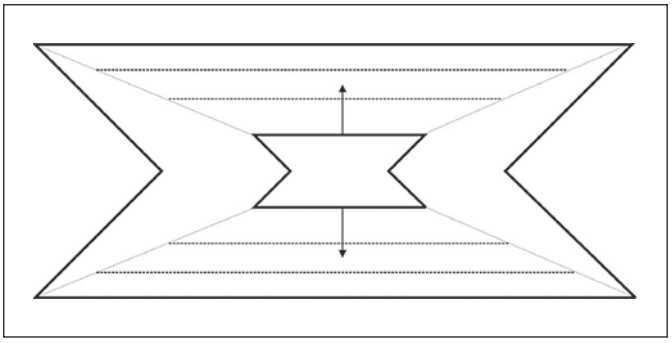

Fig. 2. Schematic of COM growth. Solid lines represent stages of growth of the crystal. Broken lines represent the growth planes of the {100} face.

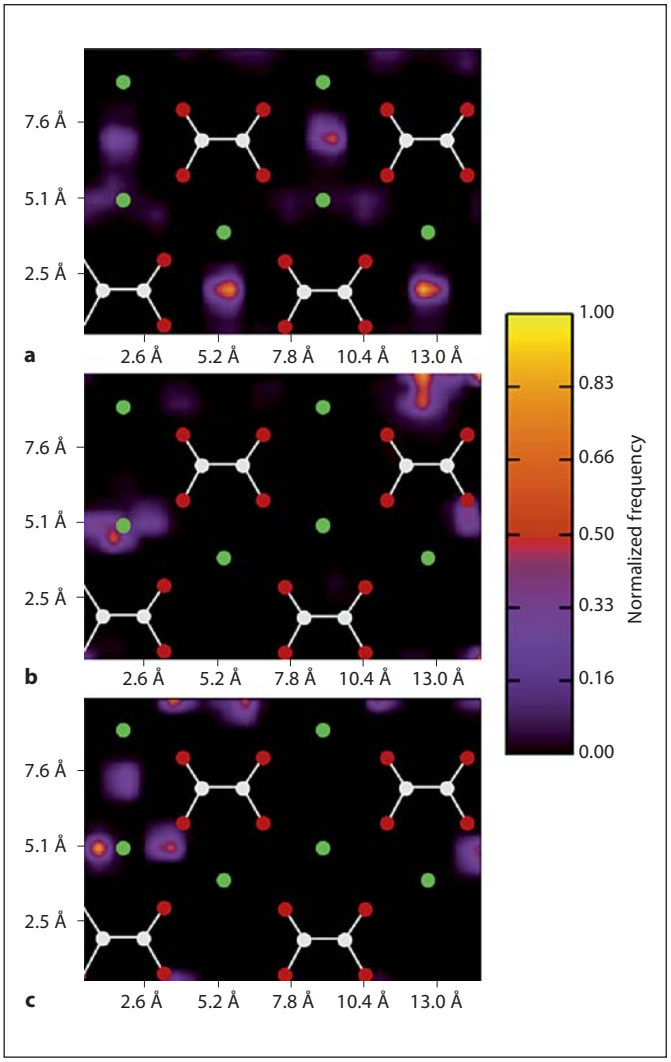

Fig. 3. Surface frequency plots derived from MD simulations. **a** Chloride ions. **b** Carboxylate oxygen atoms. **c** Phosphate oxygen atoms. Atomic coordinates are overlaid. Green represents calcium atoms, red represents oxygen atoms and white represents carbon atoms. Normalized frequency color intensity is indicated. Each plot is the sum of 9 independent simulations.

the {100} faces of COM (fig. 2). The distance between opposing {100} faces did not significantly change throughout the tested concentration range.

In comparison to P0, the P1 peptide showed considerable incorporation throughout the concentration range (fig. 1b). The distance between opposing {100} faces is negatively correlated with P1 concentration; however, no gross morphological changes in habit were observed. The incorporation pattern did not deviate across the concentration range.

Fluorescence patterns of the P3 peptide are similar to those of P1 at 0.1 and 1.0 µg/ml (fig. 1c). The distances between {100} faces at these concentrations are smaller than those of crystals grown in the presence of identical concentrations of P1. At 5.0 µg/ml of P3, COM crystals exhibit a 'dumbbell' morphology where the protein is found to be incorporated throughout the crystal with areas of higher concentration found at the center and at the longitudinal ends of the crystal. At 10.0 µg/ml, the crystal morphology was identical to that observed at 5.0 µg/ml.

To determine specific sites of adsorption on the COM {100} face, surface frequency plots were derived from MD experiments. Each experiment simulated the adsorption of a different rat bone OPN peptide to the {100} face of COM (table 1). Three atom types were observed to directly interact with the surface: chloride ions, phosphate oxygen and carboxylate oxygen.

Chloride ions were found to adsorb predominantly to the area surrounded by calcium ions and the oxygens of oxalate carboxylate groups (fig. 3a). Phosphate oxygen atoms were equally distributed between this site and 2 sites flanking the calcium ions (fig. 3c). The latter sites are equivalent. Carboxylate oxygen atoms had similar adsorptive sites as phosphate oxygen atoms. However, there was a slight preference to the sites flanking the calcium ions (fig. 3b).

Discussion

The purpose of this study was to better understand the mechanism of COM growth inhibition in the direction perpendicular to the {100} face, in the presence of phosphorylated OPN peptides. Confocal microscope images of the COM growth process showed incorporation into the growing crystal occurs for all 3 peptides used in this study. This result is similar to previous studies on the incorporation of negatively charged G protein mutants in COM [Touryan et al., 2001].

Incorporation of impurities is thought to occur by the overgrowth of the crystal lattice over the adsorbate [Davis et al., 2000]. In this scenario, the crystal would grow around the adsorbed molecule, possibly also incorporating solvent and counterions. This would introduce a defect in the crystal lattice that is likely energetically unfavorable in comparison to the formation of an ideal lattice [Davis et al., 2000]. If so, the energetic barrier to desorb an adsorbed peptide would have to be greater than the energy required to accommodate the defect. Therefore, peptides with higher adsorption energies are more likely to become incorporated into a growing crystal face. Fluorescence recovery after photobleaching experiments of the 3 peptides adsorbed to the {100} face suggest that increased peptide phosphorylation results in higher affinity [O'Young, pers. commun.]. This is in agreement with the increased crystal incorporation observed with the P1 and P3 peptides in comparison to P0.

Interestingly, overall crystal morphology was modified at the higher concentrations of P3. One possible explanation for this is the inhibition of crystal growth in other directions at these higher concentrations. Previous work has shown that P3 adsorbs to the {121} faces of COM to a lesser extent than to the {100} faces [Grohe et al., 2007]. Additionally, acidic groups have a lower interaction force with the {121} face, although still higher than with the {010} face [Sheng et al., 2005]. Perhaps at the higher levels of peptide the P3 {121} surface concentration reaches the threshold for {121} face growth inhibition.

To better understand the atomic nature of the peptide surface interaction, MD simulation trajectory analysis was performed. To provide a greater sampling, adsorption simulations of 6 distinct OPN peptides were used in addition to the previous simulations of the P0, P1 and P3 peptides. Surface frequency plots were generated to identify sites of adsorption on the COM {100} face. Three atom types were found to interact with the crystal: chloride ions, phosphate oxygens and carboxylate oxygens. This result was expected as all 3 atom types carry a negative charge in the model used. From the generated frequency plots, 3 primary sites of adsorption were identified. One site was encircled by ions and the other 2 were flanking a cationic calcium ion (fig. 3). The 2 flanking sites are equivalent. Although all 3 atom types exhibited some degree of affinity for each site, the preference of each type was markedly different.

For chloride ions, cationic and anionic atoms encircled the preferred binding site. This site is expected for a point charge, as there is symmetric attraction and repulsion from cationic and anionic species. The sites flanking the calcium atoms were only weakly occupied by chloride. This apparent weak interaction might be explained by the asymmetry of the surface atoms not directly in contact with a chloride ion residing at this secondary site.

Phosphate oxygen atoms showed no preference for any of the 3 sites. Once again, this result is expected as the spacing of the 3 sites corresponds to the distance between oxygen atoms of the phosphate ion model employed in the simulations, approximately 2.5 Å. This result also suggests that phosphate groups can directly interact with the {100} surface. However, the energy involved in this interaction is unknown. Similarly, carboxylate oxygen atoms have an adsorption site preference corresponding to its geometry. In this case, the preferential sites were those flanking the calcium ion. An interesting feature of the phosphate and carboxylate oxygen plots is the apparent structural specificity. The plots for both these atom types strongly suggest surface interactions complementary to the atomic structure of the adsorbed group.

A better understanding of the surface adsorption characteristics of individual residues can be a valuable

tool in the design of mineral growth-modulating agents. A recent study has demonstrated the binding of a peptide designed to adopt a structure that adsorbed to a hydroxyapatite surface [Capriotti et al., 2007]. The present study further characterizes the {100} surface of COM, revealing specific geometries for carboxylate and phosphate adsorption.

In conclusion, increased phosphorylation of the rat OPN 220–235 peptide results in increased adsorption to the {100} faces of COM that, in turn, results in increased crystal incorporation and inhibition in the direction perpendicular to {100}. Knowledge of the geometries of adsorptive constituents on surfaces can be used in conjunction with mathematical methods to aid in the discovery of peptides with high adsorption characteristics. This paradigm of computer-assisted design can be extended to other biomineral systems to design potent reagents that are capable of controlling crystal formation.

Acknowledgements

These studies were supported by the Canadian Institutes of Health Research, the Natural Sciences and Engineering Research Council and the Shared Hierarchial Academic Research Computing Network.

References

Burton, W.K., N. Cabrera, F.C. Frank (1951) The growth of crystals and the equilibrium structure of their surfaces. Philos Trans R Soc London Ser A *243:* 299.

Capriotti, L.A., T.P. Beebe, J.P. Schneider (2007) Hydroxyapatite surface-induced peptide folding. J Am Chem Soc *129:* 5281–5287.

Coe, F.L., J.K. Parks, J.R. Asplin (1992) The pathogenesis and treatment of kidney stones – medical progress. N Engl J Med *327:* 1151–1152.

Davis, K.J., P.M. Dove, J.J. De Yoreo (2000) The role of magnesium as an impurity in calcite growth. Science *290:* 1134–1137.

Grohe, B., J. O'Young, A. Ionescu, G. Lajoie, K. A. Rogers, M. Karttunen, H.A. Goldberg, G.K. Hunter (2007) Control of calcium oxalate crystal growth by face-specific adsorption of an osteopontin phosphopeptide. J Am Chem Soc *129:* 14946–14951.

Hoyer, J.R., J.R. Asplin, L. Otvos (2001) Phosphorylated osteopontin peptides suppress crystallization by inhibiting the growth of calcium oxalate crystals. Kidney Int. *60:* 77–82.

Keykhosravani, M., A. Doherty-Kirby, C. Zhang, D. Brewer, H.A. Goldberg, G.K. Hunter, G. Lajoie (2005) Comprehensive identification of posttranslational modifications in rat bone osteopontin by mass spectrometry. Biochemistry *44:* 6990–7003.

Nakagawa, Y., V: Abram, F.J. Kezdy, E.T. Kaiser, F.L. Coe (1983) Purification and characterization of the principal inhibitor of calcium oxalate monohydrate crystal growth in human urine. J Biol Chem *258:* 12594–12600.

Taller, A., B. Grohe, K.A. Rogers, H.A. Goldberg, G.K. Hunter (2007) Specific adsorption of osteopontin and synthetic polypeptides to calcium oxalate monohydrate crystals. Biophys J *93:* 1768–1777.

Touryan, L.A., R.H. Clark, R.W. Gurney, P.S. Stayton, B. Kahr, V. Vogel (2001) Incorporation of fluorescent molecules and proteins into calcium oxalate monohydrate single crystals. J Cryst Growth *233:* 380–388.

Sheng, X., T. Jung, J.A. Wesson, M.D. Ward (2005) Adhesion at calcium oxalate crystal. surfaces and the effect of urinary constituents. Proc Nat Acad Sci USA *102:* 267–272.

Shiraga, H., W. Min, W.J. VanDusen, M.D. Clayman, D. Miner, C.H. Terrell, J.R. Sherbotie, J.W. Foreman, C. Przysiecki, E.G. Nielson, J.R. Hoyer (1992) Inhibition of calcium oxalate crystal growth in vitro by uropontin: another member of the aspartic acid-rich protein superfamily. Proc Natl Acad Sci USA *89:* 426–430.

Wesson, J.A., R.J. Johnson, M. Mazzali, A.M. Beshensky, S. Stietz, C. Giachelli, L. Liaw, C.E. Alpers, W.G. Couser, J.G. Kleinman, J. Hughes (2003) Osteopontin is a critical inhibitor of calcium oxalate crystal formation and retention in renal tubules. J Am Soc Nephrol *14:* 139–147.